ISSN 0020-1685, Inorganic Materials, 2012, Vol. 48, No. 10, pp. 971–976. © Pleiades Publishing, Ltd., 2012.
Original Russian Text © L.A. Zemnukhova, A.E. Panasenko, G.A. Fedorishcheva, A.M. Ziatdinov, N.V. Polyakova, V.G. Kuryavyi, 2012, published in Neorganicheskie Materialy, 2012, Vol. 48, No. 10, pp. 1097–1102.

Properties of Silicon Prepared from Plant Raw Materials

L. A. Zemnukhova, A. E. Panasenko, G. A. Fedorishcheva, A. M. Ziatdinov, N. V. Polyakova, and V. G. Kuryavyi

Institute of Chemistry, Far East Branch, Russian Academy of Sciences, pr. Stoletiya Vladivostoka 159, Vladivostok, 690022 Russia

e-mail: panasenko@ich.dvo.ru

Received December 21, 2011

Abstract—High-purity X-ray amorphous silicon dioxide samples have been prepared by hydrolyzing silicon-containing plants in a 0.1 N HCl solution, followed by calcination at 700°C in air. Reducing the silica with metallic magnesium, we obtained silicon, which was then purified by sequential washings with hydrochloric, hydrofluoric, and sulfuric acids and water. The fine silicon powder thus prepared, up to 97.6% in purity, ranging in color from light brown to dark brown, was characterized by X-ray diffraction and IR spectroscopy. According to total external reflection X-ray fluorescence, electron probe microanalysis, and chemical analysis data, the major impurities in the powder were silicon dioxide, iron (within 0.45%), titanium (within 0.10%), calcium (within 0.088%), and manganese (within 0.031%). According to scanning electron microscopy data, the silicon obtained has the form of spongy material ranging in pore size from 50 to 200 nm.

DOI: 10.1134/S0020168512100159

INTRODUCTION

Most technologies in solar power engineering, which is developing very rapidly, utilize silicon. The large-scale use of silicon solar cells for power conversion depends on the availability of inexpensive polycrystalline silicon of controlled purity.

A traditional silicon source is mineral raw materials, usually quartz. Potentially attractive alternatives are silicon-containing plants. Their advantages are rapid reproduction and the possibility of extracting high-purity silicon.

Among all the types of silicon-containing plant raw materials, the most attractive silicon source is rice husk, which is present in large amounts as waste in rice processing facilities. It contains 13 to 29% ash, depending on the type, climate, and region. Rice husk ash consists predominantly of amorphous silicon dioxide (silica), with a small percentage of alkali-metal and other compounds, which can readily be removed by acid washing [1–4]. SiO_2 content can reach 99% and more, depending on processing conditions. Other siliceous plants are some cereals, horsetails, and conifers.

Silicon is typically extracted from plant raw materials in the form of silica. Silica can be reduced to elemental silicon by a variety of techniques. Metallurgical-grade silicon (about 98% purity) is commonly produced by carbothermic reduction of quartz in electric arc furnaces at ~1900°C. It can also be produced by metallothermic reduction using metals such as magnesium, calcium, barium, and aluminum as reductants [2, 5, 6]. Magnesiothermic reduction is potentially attractive for the preparation of high-purity silicon because this process includes rather simple purification steps and is relatively cheap.

The objectives of this work were to prepare silicon dioxide from various types of silicon-containing plant raw materials (rice straw and husk, larch needles, and horsetail stems), convert it to elemental silicon through magnesiothermic reduction, and study their properties using chemical analysis, electron probe microanalysis, X-ray diffraction (XRD), IR spectroscopy, electron paramagnetic resonance (EPR), and scanning electron microscopy (SEM).

EXPERIMENTAL

The following plant raw materials, collected in different regions of Primorskii krai, were used as silicon sources:

rice (Oryza Sativa; Dal'nevostochnyi rice husk; Darii-8, Lugovoi, and Khankaiiskii-52 rice straw);

sylvan horsetail (Equisetum hyemale) and scouring horsetail (Equisetum sylvaticum); and

larch needles (Larix dahurica).

For comparison, we investigated silica samples of mineral origin: the mineral diatomite from Australia and hydrous silicic acid, $SiO_2 \cdot nH_2O$ (RF State Standard GOST 4214-78).

The plant raw materials were treated with a hydrochloric acid solution and then calcined as described elsewhere [7]. This procedure yielded amorphous silica.

Table 1. Characteristics of silica samples

No	Raw materials		Percentage					
	Type	Ash yield, %	SiO_2	Fe_2O_3	TiO_2	CaO	MnO	H_2O
1	Dal'nevostochnyi rice husk	15.0	99.40	0.13	0.08	0.15	0.02	0.5
2	Darii-8 rice straw	12.3	97.54	0.41	0.26	0.89	0.15	1.1
3	Lugovoi rice straw	11.5	93.65	0.10	0.04	0.83	0.08	<0.1
4	Khankaiskii-52 rice straw	15.3	90.96	0.29	0.19	0.93	0.19	<0.1
5	Larch needles	4.3	83.66	0.84	0.45	5.48	0.324	1.7
6	Scouring horsetail	10.2	89.62	0.17	0.09	2.28	0.012	0.6
7	Sylvan horsetail	10.2	91.24	0.28	0.13	1.11	0.053	0.6
8	Diatomite	–	67.03	2.66	0.53	0.53	0.006	14.0
9	$SiO_2 \cdot nH_2O$ reagent	–	88.40	0.04	0.24	0.05	–	11.6

The silicas prepared from plant or mineral raw materials were ground with metallic magnesium powder (10% excess of magnesium). The mixture was compacted in a ceramic crucible and then ignited either using a nichrome electric fuse or by heating in a muffle furnace to 650–700°C. The initiation of combustion was followed by exothermic formation of elemental silicon:

$$SiO_2 + 2\ Mg \rightarrow Si + 2\ MgO.$$

The combustion process ceased after 5–15 min.

To remove by-products (magnesium silicate, magnesium silicide, and magnesium oxide) and unreacted substances from the silicon thus obtained, it was sequentially washed with a hydrochloric acid solution, a mixture of sulfuric and hydrofluoric acids, and water as described by Banerjee et al. [6].

Table 2. Actual yield and purity of synthesized silicon

Sample no.	Si yield, %	Percent impurities			
		Fe	Ti	Ca	Mn
1	40.8	0.09	0.029	0.005	0.004
2	43.0	0.18	0.026	0.038	0.010
3	42.3	0.064	0.054	0.047	0.031
4	61.9	0.022	0.036	0.003	0.008
5	55.7	0.45	0.10	0.088	0.004
6	62.7	0.24	0.038	0.079	0.002
7	62.9	0.33	0.082	0.026	0.007
8	33.6	–	0.13	0.003	0.001
9	9.7	0.14	0.24	–	0.0005

The silica and silicon samples obtained were identified by XRD and IR spectroscopy. XRD patterns were collected on a Bruker D8 ADVANCE diffractometer with CuK_α radiation. IR spectra were measured in the range 400–4000 cm^{-1} on a Shimadzu FTIR Prestige-21 Fourier transform spectrometer. Electron micrographs were obtained on a JEOL JSM-7700F scanning electron microscope equipped with a JED 2300 energy dispersive X-ray microanalysis system. The concentration of impurities was determined by total external reflection X-ray fluorescence (TER XRF) analysis on a TXRF 8030C spectrometer.

The presence and structural characteristics of paramagnetic impurities were inferred from EPR data. EPR spectra of samples of the same weight were measured on a Bruker EMX 6.1 standard X band spectrometer at an rf modulation amplitude of 0.5 mT and a microwave power of 20 mW. The *g*-factors of EPR lines were calibrated against that of the conduction electron spin resonance line of metallic lithium nanoparticles in a LiF:Li standard (the width and *g*-factor of this signal are ~0.027 mT and 2.002293 ± 0.000003, respectively). According to preliminary results, evacuating the samples to $\sim 1.3 \times 10^{-4}$ Pa causes no significant changes in their EPR spectra, which suggests that the so-called oxygen effect was negligible.

RESULTS AND DISCUSSION

Plant raw materials as silicon sources have a number of important advantages: reproducibility and the facts

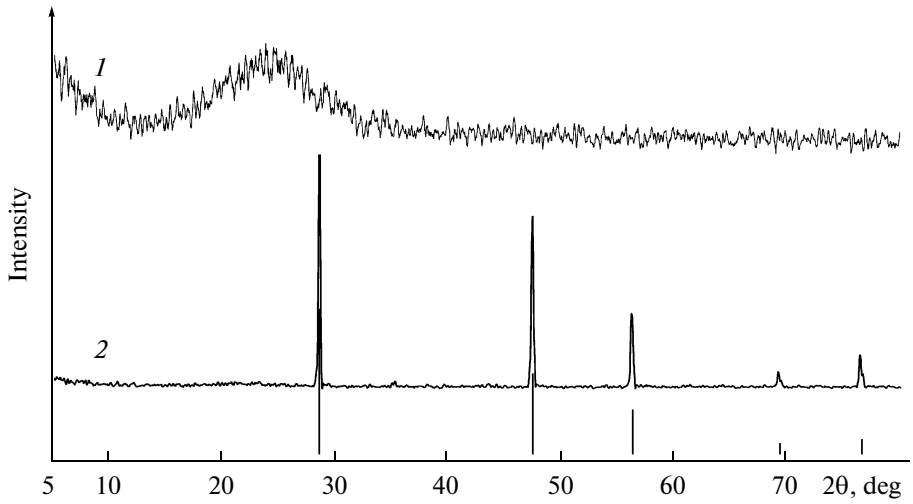

Fig. 1. XRD patterns of (*1*) plant-derived silica and (*2*) elemental silicon obtained from it.

that they are by-products in the agricultural and forestry engineering industries and that the resulting silica is amorphous. A key parameter of plant raw materials is the silica content, which can reach 22% (Table 1).

After the removal of mineral salts and organics from plant raw materials through acid hydrolysis and subsequent calcination, as described elsewhere [7], the residue is amorphous silica. The purity of the SiO_2 thus prepared ranges from 83.7 to 99.4%. According to TER XRF data, the major impurities in the silica samples obtained are iron, titanium, calcium, and manganese (Table 1).

The silicon produced through magnesiothermic reduction of plant-derived silica ranges widely in yield. The actual yield of the reduction reaction varied from run to run and depended on the type of silica (Table 2). In addition, the reaction yield depended on how the starting mixture was ignited. When ignition was ensured by heating the crucible and mixture, the reaction yield was a factor of 1.5–2 lower than in the case of ignition with an electric fuse.

As seen from Table 2, the reduction reaction is most effective in the case of the silica prepared from rice straw and horsetail. Clearly, rice straw is far more convenient for the implementation of the silicon preparation process because it is abundant rice processing waste.

Figures 1 and 2 show XRD patterns and IR spectra of the synthesized silicon in comparison with silicon dioxide. In the IR spectrum of elemental silicon, silicon proper is represented only by the band at 465 cm^{-1} [8], which overlaps with the bending band of the Si–O–Si group in SiO_2 [7]. All of the other bands seem to arise from silica impurities.

The purity of the silicon prepared from plant raw materials is 97.6%. The major impurities are silicon dioxide (up to 2.15%), iron (0.022–0.45%), titanium (0.026–0.10%), calcium (0.003–0.088%), and manganese (0.002–0.031%).

The EPR spectrum of the SiO_2 sample (Table 1, sample 1) prepared from rice husk shows two lines: a narrow line with an effective value $g_1 \approx 4.3$ and a considerably stronger, broad line with an effective value $g_3 \approx 2.05$ (Fig. 3, spectrum *2*). According to calculation results and modeling of the EPR spectra of $3d^5$ ions in noncrystalline materials [9, 10], the line at g_1 is due to isolated Fe(III) and/or Mn(II) ions in their high-spin state, situated in a severely distorted octahedral or tetrahedral crystal field. At the same time, the fact that the line at g_3 has no hyperfine sextet, in contrast to what is

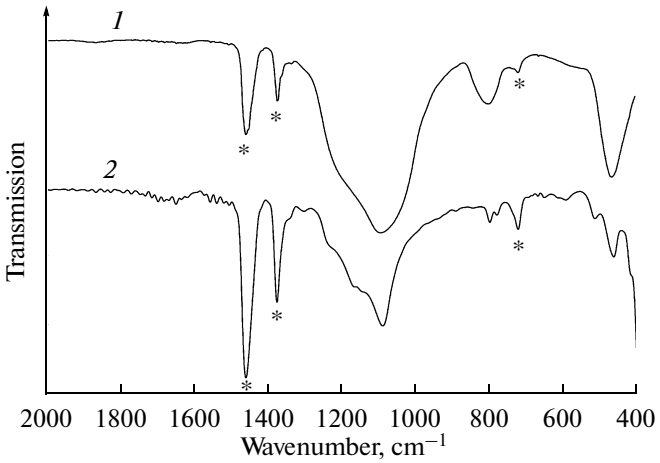

Fig. 2. IR spectra of (*1*) silica produced from rice straw and (*2*) elemental silicon obtained from it.

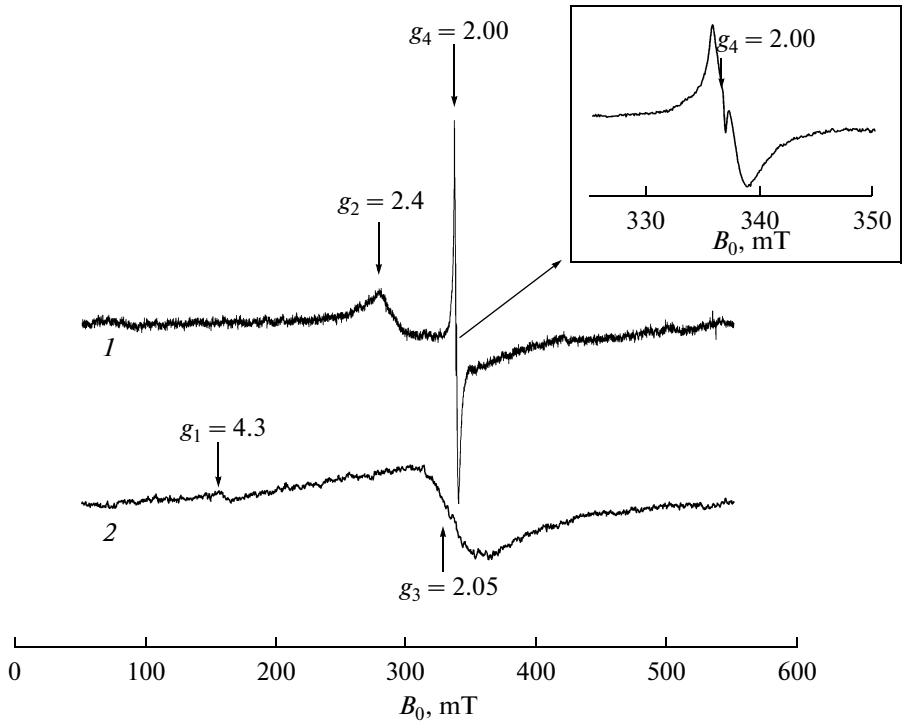

Fig. 3. Room-temperature EPR spectra of (*1*) silicon and (*2*) silicon dioxide.

typical of Mn(II), suggests that the spectrum is predominantly due to Fe(III) ions. The line at g_3 in noncrystalline materials is commonly attributed to isolated high-spin Fe(III) ions in a slightly distorted octahedral crystal field [9–12].

However, this point of view is not generally accepted. For example, Moon et al. [13] think that this line arises from clusters containing two or more exchange-coupled Fe(III) ions.

The EPR spectrum of the silicon (Table 2, sample 1) prepared from SiO_2 (Table 1, sample 1) extracted from rice husk contains an asymmetric strong line with an effective value $g_2 \approx 2.4$ and a narrow line with an effective value $g_4 \approx 2.00$ (Fig. 3, spectrum *1*). The line at g_4 has a structure (Fig. 3 inset) typical of crystalline powders containing Fe(III) impurities [14]. The above characteristics of the line at g_4 strongly suggest that it arises from Fe(III) ions in a slightly distorted octahedral or tetrahedral crystal field.

The effective value of the *g*-factor, significant asymmetry, and large width of the line at g_2 indicate that it arises from Fe(III) ions in a noncrystalline phase. At the same time, comparison of the shape and parameters of the line at g_2 with those of lines in the spectrum of SiO_2 (Fig. 3, spectrum *2*) demonstrates that the noncrystalline phases in these samples differ markedly in structure.

Thus, the EPR spectrum of elemental silicon indicates that the synthesized silicon sample contains, in addition to a crystalline phase, a noncrystalline phase which differs from the parent silicon dioxide. This conclusion is consistent with the IR spectroscopy data in Fig. 2.

The SEM micrographs in Figs. 4a–4c demonstrate that the silicon samples (Table 2, samples 1, 2, 5) consist largely of spongy material ranging in pore size from 50 to 200 μm. The likely cause of the observed porosity is that acids leach out magnesium compounds and SiO_2 from the reduction product, thereby producing voids [5]. Like in previous work [15], the silicon prepared from rice straw has a cellular structure with an average pore diameter of 1.5 μm (Fig. 4b). There is general belief that it is the porous structure of silicon which makes it possible to effectively remove—using acids—not only metallic impurities from the particle surface but also elements capable of penetrating deep into particles, such as boron, phosphorus, carbon, and oxygen [15]. In one silicon sample (Table 2, sample 4), we observed the formation of silicon rods 20–100 nm in diameter and up to 300 nm in length on the surface of rounded particles about 5 μm in diameter (Fig. 4d). The formation of similar structures was reported earlier by Noskova et al. [16].

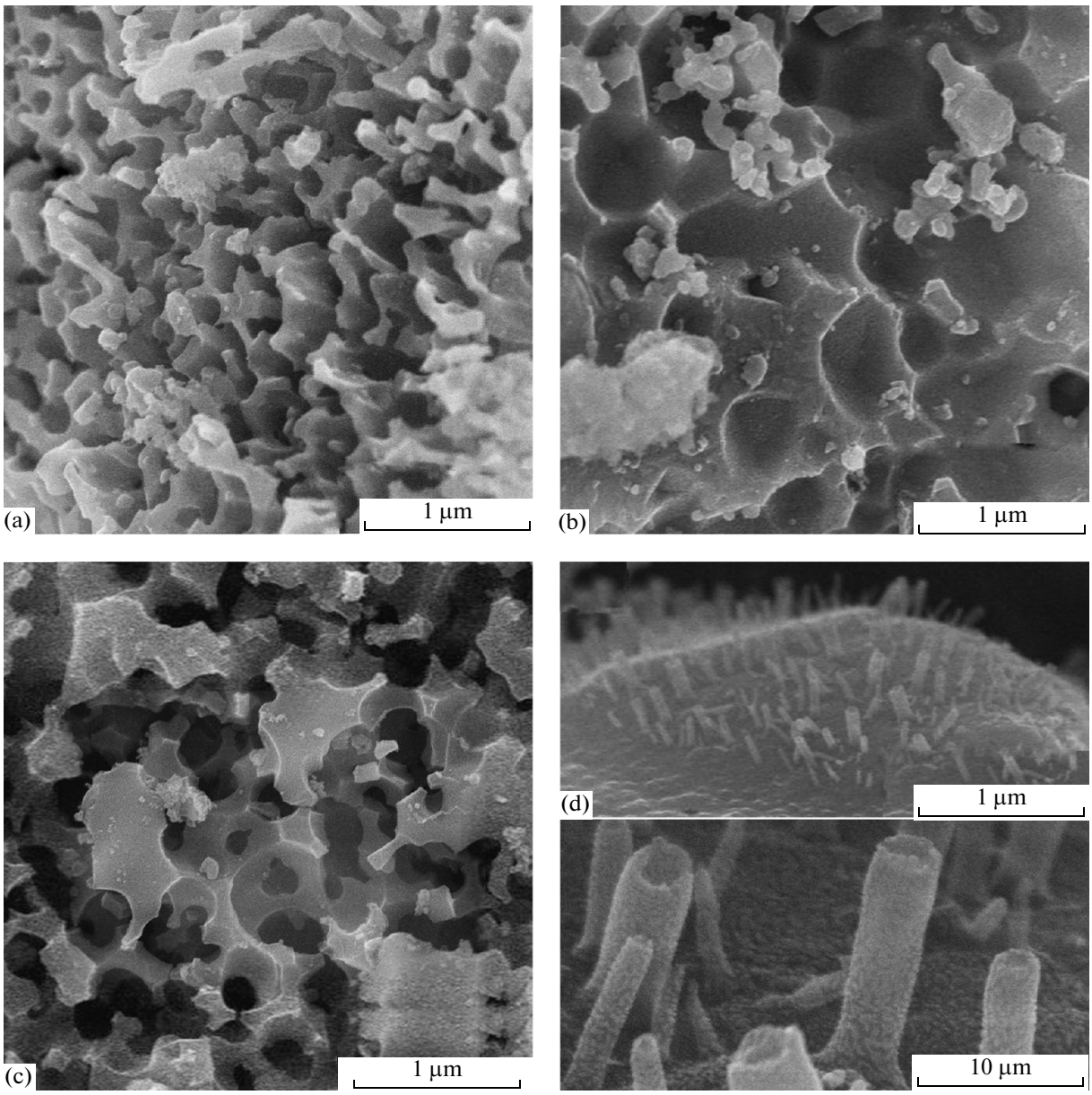

Fig. 4. Micrographs of silicon samples prepared from plant raw materials: (a) rice husk, (b, d) rice straw, (c) larch needles.

CONCLUSIONS

Silicon prepared by metallothermic reduction of silica produced from rice husk is pure enough for further purification steps and can be used as a starting material for the production of solar-grade and semiconductor silicon. The use of an electric fuse increases the silicon yield in comparison with the initiation of combustion in a muffle furnace.

The silicon obtained in this study has a porous structure and can be purified by acids to remove by-products, which ensures almost complete dissolution of metallic and nonmetallic impurities, in contrast to monolithic single-crystal, polycrystalline, or amorphous silicon prepared through melting.

REFERENCES

1. Sergienko, V.I., Zemnukhova, L.A., Egorov, A.G., et al., Sustainable Sources of Chemical Raw Materials: Combined Processing of Rice and Buckwheat Production Waste, *Zh. Ross. Khim. O–va. im. D. I. Mendeleeva*, 2004, vol. 48, no. 3, pp. 116–124.
2. Swatsitang, E., Srijaranai, S., and Arayarat, P., Preparation of Silicon from Rice Hulls, *Technical Digest of the International PVSEC-14*, 2004, p. 301.
3. Pukird, S., Chamninok, P., Samran, S., et al., Synthesis and Characterization of SiO_2 Nanowires Prepared from

Rice Husk Ash, *J. Met. Mater. Miner.*, 2009, vol. 19, no. 2, pp. 33–37.

4. Ghasemi, Z. and Younesi, H., Preparation and Characterization of Nanozeolite NaA from Rice Husk at Room Temperature without Organic Additives, *J. Nanomater.*, 2011, paper ID 858 961.
5. Swatsitang, E. and Krochai, M., Preparation and Characterization of Silicon from Rice Hulls, *J. Met. Mater. Miner.*, 2009, vol. 19, no. 2, p. 91.
6. Banerjee, H.D., Sen, S., and Acharya, H.N., Investigations on the Production of Silicon from Rice Husk by the Magnesium Method, *Mater. Sci. Eng.*, 1982, vol. 52, pp. 173–179.
7. Zemnukhova, L.A., Egorov, A.G., Fedorishcheva, G.A., et al., Properties of Amorphous Silica Produced from Rice and Oat Processing Waste, *Inorg. Mater.*, 2006, vol. 42, no. 1, pp. 24–29.
8. Shen, S.C., Fang, C.J., Cardona, M., and Genzel, L., Far-Infrared Absorption of Pure and Hydrogenated a-Ge and a-Si, *Phys. Rev. B*:, 1980, vol. 22, no. 6, pp. 2913–2919.
9. Nicklin, R.C., Farach, H.A., and Poole, C.P., EPR of Mn^{2+}, Fe^{3+}, and Cu^{2+} in Glasses of the Systems BaO–B_2O_3–Al_2O_3 and CaO–B_2O_3–Al_2O_3, *J. Chem. Phys.*, 1976, vol. 65, no. 8, pp. 2998–3005.
10. Fucheng, L., The EPR of Fe^{3+} and Mn^{2+} in Glasses and Their Site Symmetries, *Sci. China A,* 1982, vol. 25, no. 12, pp. 1298–1304.
11. Toderas, M. and Ardelean, I., EPR Investigation of Manganese Ions in $B_2O_3 \cdot$ BaO Glass Matrix, *J. Optoelectron. Adv. Mater.*, 2007, vol. 9, no. 3, pp. 629–632.
12. Ardelean, I., Andronache, C., Cimpean, C., and Pascuta, P., EPR and Magnetic Investigation of Calcium-Phosphate Glasses Containing Iron Ions, *J. Optoelectron. Adv. Mater.*, 2006, vol. 8, no. 4, pp. 1372–1376.
13. Moon, D.W., Aitken, J.M., MacCrone, R.K., and Cieloszyk, G.S., Magnetic Properties and Structure of $x$$Fe_2O_3$–(1 – x)BaO, $4B_2O_3$ Glasses, *Phys. Chem. Glasses*, 1975, vol. 16, pp. 91–96.
14. Weil, J. and Bolton, J.R., *Electron Paramagnetic Resonance: Elementary Theory and Practical Applications*, New Jersey: Wiley–Interscience, 2007.
15. Won, C.W., Nersisyan, H.H., and Won, H.I., Solar-Grade Silicon Powder Prepared by Combining Combustion Synthesis with Hydrometallurgy, *Sol. Energy Mater. Sol. Cells*, 2011, vol. 95, pp. 745–750.
16. Noskova, N.I., Churbaev, R.V., Vil'danova, N.F., et al., Structure and Microhardness of Nanocrystalline Al- and Ti-Based Composite Alloys, *Fundam. Probl. Sovrem. Materialoved.*, 2009, vol. 6, no. 2, pp. 54–62.

SPELL: OK